Symmetric longitudinal Mach-Zehnder modulator using lithium niobate

Sadeq Adnan Hbeeb, Ahmad S. Abdullah, Haider Ali Jasim Alshamary
Department of Communication Engineering, College of Engineering, University of Diyala, Diyala, Iraq

Article Info

Article history:

Received Jul 5, 2022
Revised Oct 13, 2022
Accepted Oct 24, 2022

Keywords:

Lithium niobate
Longitudinal configuration
Mach-Zehnder interferometer
Push-pull (dual-drive controlled)
Symmetric electro-optic modulator

ABSTRACT

There are many problems that restrict the work of the Mach-Zehnder modulator (MZM), including the lack of using various windows of wavelengths, the large half-wave voltage, and the small optical confinement factor. In this paper, a mathematical model for MZM based on lithium niobate (LN) is designed to solve these problems. In this model, a wide window of optical wavelength from visible-to-infrared (632.8-to-1560 nm) was utilized. Moreover, it achieved a better modulation with lower attenuation and a lower dispersion by the window (1550-1560) nm. The other window of optical wavelength is about (632.8-to-634 nm), and (646-to-647 nm) which can be used for short-haul applications to reduce attenuation and dispersion. Furthermore, a small length of the arm, about 2-3 mm, was utilized to accomplish a large change of the refractive index and lower applied voltage of up to 250 V. The small operation half-wave voltage achieved about 1.2 V leading to better switching of the MZM. In addition, a large optical confinement factor of ≤1 unitless was obtained. Even better performance of MZM was attained by using a suitable length arm of MZM of about 2 mm, along with an electric field of about 175 V/mm and 233 V/mm using poling at 100 V.

Corresponding Author:

Ahmad S. Abdullah
Department of Communication Engineering, University of Diyala
Baqubah, 32001 Diyala, Iraq
Email: ahmed.alogaidi28@gmail.com

1. INTRODUCTION

Lithium niobate (LN) contains preferred specifications among other materials. The broad transparent band of LN fabric provides about 4.6-340 µm that can be applicable for a variety of applications in visible to mid infrared wavelength windows [1]–[3]. Soft dispersion with lower absorption losses of smaller than 0.15%/cm can be achieved through the wavelength of 1.06 µm. Consequently, LN is becoming essential for challenging implementations such as modulation of wideband devices of high-bit long haul optical telecommunications [4], body of LN [5], [6] that extends for greater broadband frequencies, in the Mach-Zehnder interferometer (MZI) configuration, and modulators of imprinted LN [7]–[9]. Lately, LN insulator membranes (LNOI) have appeared as a promising platform for forming well-contained waveguide devices (i.e., better confinement factor) [10]–[12]. Meantime, LNOI modulators with ultra-high EO bandwidth and low drive voltage have recently been established [13], [14]. Non-centrosymmetric fabrics are well recognized for exhibiting second-order electrical sensitivity. Electro-optic effects together with non-linear effects and Pockel effects were used for a wide spectrum of applications such as quantum photonics, devices of optical communications, safety, aviation, and biology [15]–[18]. LN is utilized in many applications because of the big second-order electrical sensitivity, among other things, which can afford effective and high-speed modulation for electro-optic systems [19]. In comparison to LN [17], silicon nitride

SiN is centrosymmetric, affecting pockel-based modulation in the waveguide center itself [20], [21]. Moreover, compared to semiconductors that electrically modulate light absorption across the impact of Franz-Keldysh, the modulator of LN modifies the intensity of light without phase disturbance, i.e. without chirping. Thus, despite the excellent achievements of semiconductors in systems of short-haul telecommunications, the modulation with no chirping supplied using LN-based parts remains protected through its transmission of high-bit rate optical signal via long-haul telecommunication [22], [23]. It has been shown, for almost two decades, that after surface stimulation [24], [25], the silicon surrounded the fabric of the thin substratum of the LN, and several accounts of the modulators by thin substratum LN were released by electro-optic effect [7], [13], [26]. Complicated wave guiding systems can be constructed with one surrounding coating and various perpendicular changes. That can be done by utilizing one silicon coating lithography to regulate the light route below the surrounding LN area in addition to the two ends of sides of the surrounding region [27]. Controllable resonator rings [28], switches [26], modulators in separate phases [29]–[31], and MZI [32], [33] are noteworthy instruments using the elevated variation of the index which used a thin substratum of the LN. Different hybrid systems, which depend on Si_3N_4 or Si [18], [34] to load and guide an optical mode, are developed by conjunction. A prevalent theme among these systems owns a decreased mode volume. Therefore, it results in significantly increased electro-optical efficiency in comparison to its predecessors in large volumes. Then, a half-wave voltage is mainly reduced. Thus, the significantly reduced application of perfect footprint is an advanced optic technique. This is due to the reduced products of half wave voltage duration combined across the ability to control the variance of high indexes of guides. In addition, the thin substratum of the LN up to this point is the material system's considerably reduced permittivity and this is the main advantage of this technique [31], [35], [36]. Rao and Fathpour [14] intended a theoretical work by LN for the MZI modulator. This modulator worked with deferential arm lengths of approximately 2 and 10 cm, with a low half wave voltage of about 1 volt. This reference used a large length of arms (i.e., length of arm in cm) reflecting a large size device and a low applied half-wave voltage.

In this paper, the LN symmetrical push-pull MZI modulator is introduced with different lengths of the arm of approximately 2, 3, and 10 mm. Therefore, the presented design offers a low small size device with a low half-wave voltage of about 1.2 V. The size of the length arm of MZM is an effective factor because decreasing the length of the arm due to increasing relative refractive index difference leads to achieving better modulation. The previously mentioned reference used a length of arm in cm, while this paper uses the length of arm in mm. At the same time, the proposed design in this paper uses a wide window of optical wavelength from visible-to-infrared (i.e, 633-1560 nm), while in the compared reference a wide window of optical wavelength is not applied. Moreover, in [14], the arms are equal in length or not imbalance and hence the delay time is never inducing between arms, and the optical path difference between arms is the same and the optical delay is not found.

2. RESEARCH METHOD

2.1. Symmetrical push-pull MZIM

A MZI push-pull modulator is symmetric because the length of the arms for the waveguide are equal in length. Therefore, the optical path difference for arms is the same. An applied voltage is driven on both sides of the waveguide (i.e., dual drive voltage), accordingly, the MZIM is called a push-pull, as shown in Figure 1. In this work, the longitudinal modulator is introduced so that the mechanism of this modulator is represented by applying a voltage in parallel to the direction of the transmitting light in the modulator.

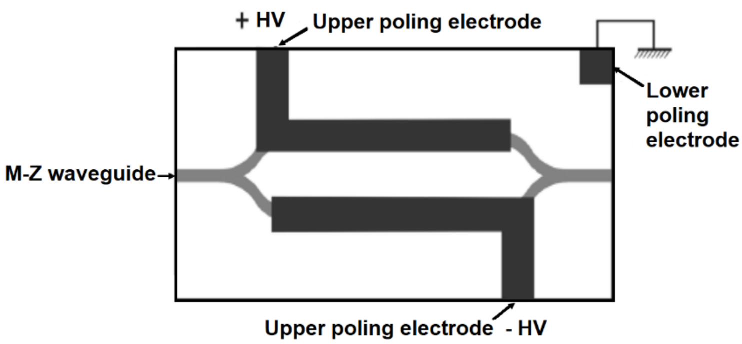

Figure 1. Symmetric push-pull MZIM

The fundamental concept of an electro-optic device changes the optical properties of a material with an applied voltage [37]. These changes result in a change in the refractive index Δn of material by applying an electric field on the material of crystal [38].

$$\Delta n = \frac{1}{2} n_o^3 r E \quad (1)$$

Where, n_o is the ordinary refractive index, r is electro-optic coefficient, and E is the electric field for longitudinal modulator $E = \frac{V}{L}$, where V is applied voltage and L is the length of arm for MZM modulator.

A technique of phase modulator (longitudinal phase modulator) is presented in this study, as shown in Figure 2. Where an electrical field is applied across the axes of the crystal. The polarized light along the axis suffers from the change of refractive index, which is related to the applied electrical field. Therefore, phase modulation induces, and the phase shift can be calculated using [38].

$$\Delta\emptyset = \frac{2\pi}{\lambda} \Delta n L \quad (2)$$

Where ΔØ is a phase difference, λ is the optical wavelength, Δn is relative refractive index difference, and L is the length of the arm modulator. Thus, the $\Delta\emptyset$ for longitudinal phase modulator is [29].

$$\Delta\emptyset = \frac{\pi}{\lambda} n_o^3 r V \quad (3)$$

Where, n_o^3 is the ordinary refractive index, r is the electro-optic coefficient and V is the applied voltage. The half-wave voltage is the voltage required for a 180° phase change (i.e. $\Delta\emptyset = \pi$). Therefore, the half-wave voltage V_π for the ordinary longitudinal phase modulator is [38].

$$V_\pi = \frac{\lambda}{n_o^3 r} \quad (4)$$

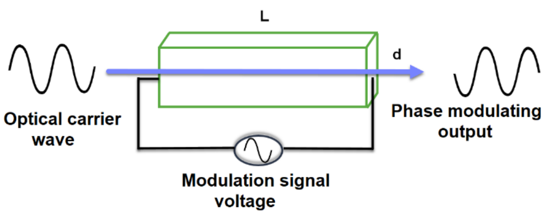

Figure 2. Longitudinal electro-optical modulator LN crystal

A design of the symmetrical push-pull MZIM is shown in the supplementary material and in Table 1. In this modulator design, three regions of wavelength are accomplished: (632.8-634) nm and (646-647.5) nm, using a short-haul application. In addition, the long-haul applications achieved by the window are 1550-1560 nm. The refractive index difference depends on a low applied voltage and large wavelength.

Table 1. Wavelengths (λ), extraordinary refractive index n_e, and electro-optic coefficients (r_{33}), for LN

Wavelength (nm)	n_e	r_{33}(pm/V)	References
632.8	2.2022	31	[39], [40]
634	2.2019	30.5	[40], [41]
646	2.1993	28.5	[40], [41]
647.5	2.1991	28	[40], [41]
1550	2.1376	26	[40], [41]
1560	2.1373	25	[40], [41]

2.2. Mathematical model

In the MZI modulator, the incident light is split into two components (I_1 and I_2) with symmetric arm lengths (i.e., L_1 and L_2 are the same length). The components are combined on the end of the device (i.e.

I_{out}=I_1+I_2). Thus, if an electric field is applied longitudinally in the case of a dual drive electrode push-pull MZI modulator, then it achieves as given in (5) [14]:

$$V_\pi = \frac{\lambda n_{eff}}{\pi L n_e^4 \Gamma} \tag{5}$$

In (6), for the longitudinally uniform push-pull modulator is [38]:

$$E = \frac{2\Delta n V \pi}{\lambda} \tag{6}$$

Where, I_{out} is the output laser power in watts, I_o is initial laser power in watts, n_{eff} is the effective refractive index, n_e^4 is the extraordinary refractive index, and Γ is the confinement factor.
Hence,

$$\frac{2I_{out}-I_o}{I_o} = 2\left(\frac{2\Delta n V_\pi}{\lambda}\right)\left[\left(\frac{2\Delta n V_\pi}{\lambda}-1\right)+\left(1-\frac{2\Delta n V_\pi}{\lambda}\right)\cos\Delta\emptyset\right] \tag{7}$$

$$2I_{out} = \frac{I_o[\lambda^2+8\Delta n^2 V_\pi^2 - 4\lambda\Delta n V_\pi + K]}{\lambda^2} \tag{8}$$

$$K = (4\lambda\Delta n V_\pi - 8\Delta n^2 V_\pi^2)\cos\Delta\emptyset \tag{9}$$

$$\triangle\,\emptyset = \frac{2\pi n_{eff} L}{\lambda} - i\frac{\alpha L}{2} \tag{10}$$

The term "△ ∅" is the complex phase difference in which a power absorption loss α dB/mm can be considered [42]. Also, $\Delta\phi$ is the phase shift of the modulator with the effect of an electric field, and f_m is a modulation bandwidth.

$$\Delta\phi = \frac{\pi L r_{eff} n_{eff}^3 E}{\lambda} \tag{11}$$

$$f_m = \frac{6.84}{\alpha L_m} \tag{12}$$

Where, n_{eff} =ne, r_{eff} is effective electro-optic coefficient, E is electric field, and L_m is length of arm modulator.

$$\Delta\phi = \frac{2\pi L r_{eff} n_{eff}^3 \Delta n V_\pi}{\lambda^2} \tag{13}$$

$$2I_{out} = \frac{I_o[\lambda^2+8\Delta n^2 V_\pi^2 - 4\lambda\Delta n V_\pi + K]}{\lambda^2} \tag{14}$$

The substitution of V_π in (5) into (14) yields:

$$2I_{out} = \frac{I_o\left[\frac{\pi^2 L^2 n_e^8 \Gamma^2 \lambda^2 + 8\Delta n^2 \lambda^2 {n_{eff}}^2}{\pi^2 L^2 n_e^8 \Gamma^2} - 4\Delta n \frac{\lambda^2 n_{eff}}{\pi L n_e^4 \Gamma} + Y\right]}{\lambda^2} \tag{15}$$

$$Y = \left(4\Delta n \frac{\lambda^2 n_{eff}}{\pi L n_e^4 \Gamma} - 8\Delta n^2 \frac{\lambda^2 {n_{eff}}^2}{\pi^2 L^2 n_e^8 \Gamma^2}\right)\cos(\Delta\emptyset) \tag{16}$$

$$I_{out} = I_o[\pi^2 L^2 n_e^8 \Gamma^2 + 8\Delta n^2 {n_{eff}}^2 - 4\Delta n\, n_{eff} \pi L n_e^4 \Gamma + \left(4\Delta n\, n_{eff} \pi L n_e^4 \Gamma - 8\Delta n^2 {n_{eff}}^2\right)\cos(\Delta\emptyset)]\ (2\pi^2 L^2 n_e^8 \Gamma^2)^{-1} \tag{17}$$

These (16) and (17), reflect the model of modulation output power and output optical power, respectively, for the MZI modulator. In this paper, we used MATLAB 2018b simulation. Where the initial power laser I_o is 100 W, and the length of the arm modulator is about 2-3 mm, and 10 mm. The confinement factor Γ is 10^-4 to 1 unit less [43]. The relative refractive index difference Δn 0.009 to 0.01, effective refractive index n_{eff} is 1.0688 to 1.1011. The power absorption loss α is 0.085 to 0.12 dB/mm for L is 2, 3 mm, and α is 0.02 dB/mm for L is10 mm, also see Table 1.

3. RESULTS AND DISCUSSION

This paper suggests a mathematical model for a symmetric longitudinal push-pull MZIM. This modulator can work with a wide window of wavelength which considers the best application for high-speed optical communication systems. This device can be used for different regions of light including a visible-into-infrared region as a window (632.8-1560) nm. The presented structure shows improved modulation specifications that can convey optical signals through short or long-haul optical communication. A wavelength window (1550-1560) nm is very helpful as the optical modulated signal transmission can operate with high-quality modulation. The window is characterized by low dispersion and attenuation. Also, two windows of wavelength (632.8-634) nm and (646-647.5) nm are used with a length of modulator 2-3 mm and 10mm respectively. These windows are used for modulation of the optical signal via transmission of short haul. Therefore, the effect of attenuation and dispersion can be reduced. The small length of the modulator arm leads to a large relative refractive index difference and lower applied voltage V leading to a higher quality of modulation. The best modulation is achieved when the length of the arm is 2-3mm, if compared with 10 mm, as in (18) [44], [45] (see Figures 3(a) and (b), Figure 4, and Figures 5(a) and (b)).

$$\Delta n = -\frac{n^3 r_{41} \Gamma V}{2L} \tag{18}$$

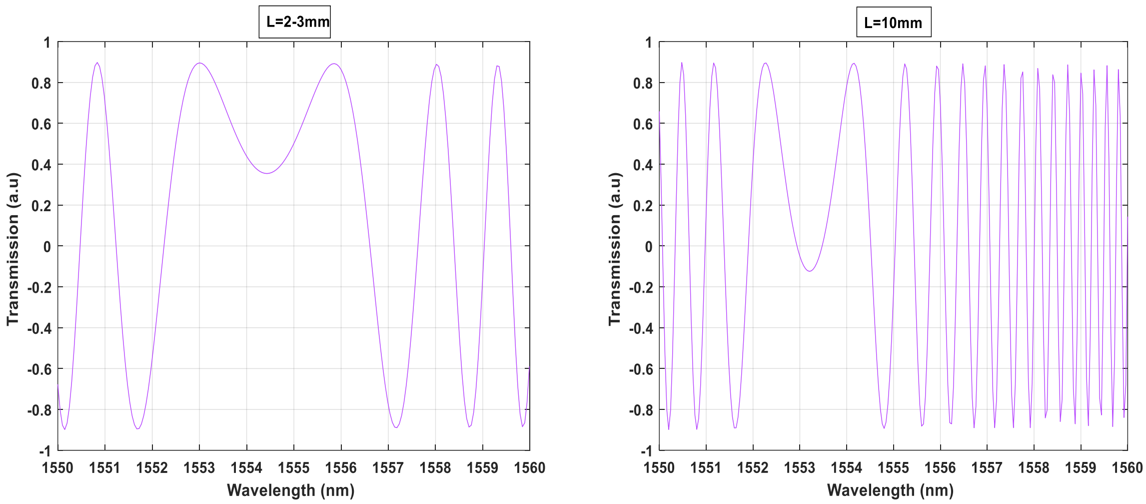

(a) (b)

Figure 3. Optical spectra of near infrared with different length of arms L (a) L=2-3 mm and (b) L=10 mm, for modulator with low dispersion and attenuation

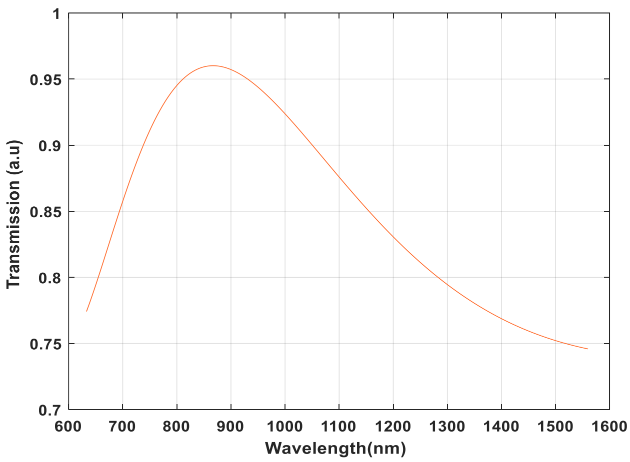

Figure 4. A window of wavelength for symmetric longitudinal MZIM

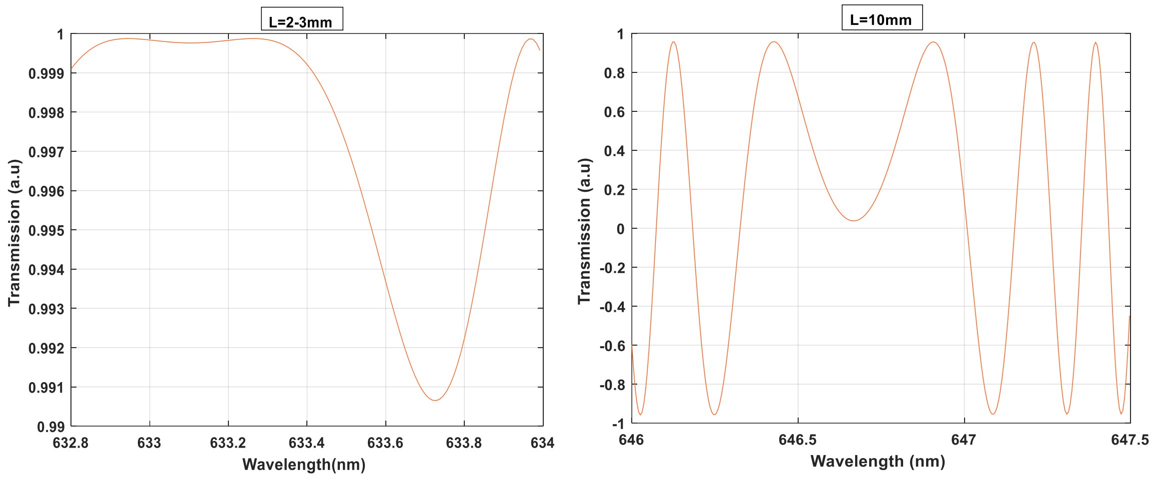

(a) (b)

Figure 5. Optical spectra of visible light with length of arms L (a) L=2-3 mm and (b) L=10 mm for modulator and using for short haul application

The refractive index difference depends on a low applied voltage and large wavelength, as in (19) and (20) [38]. The refractive index can be changed due to the control of phase modulation where the phase difference induces between arms. After this change, the induced phase shift converts from phase modulation into intensity modulation. Consequently, the phase shift depends on the applied voltage V and length of modulator arms L. In another case, the applied voltage V induces phase modulation without intensity modulation by an input polarizer. Hence the applied voltage V works as on or off. If V is on, the voltage applied and phase modulation induces, and otherwise, if the V is off, the phase modulation is not induced. The half-wave voltage $V\pi$ is considered the small part of applied voltage V. When the $V\pi$ decreases to a smaller value, this results in high quality of modulation because the half-wave voltage $V\pi$ is an effective factor to improve the electro-optical device. Thus, the operation half-wave voltage used in the value of 1.2 V.

$$\Delta\emptyset = \frac{2\pi V \Delta n}{E\lambda} \tag{19}$$

$$\Delta n = \frac{\Delta\phi E\lambda}{2\pi V} \tag{20}$$

The driving voltage for the modulator represents a suitable value (i.e., 250 V) as it gives a better performance for the modulator using a half-wave voltage about 1 V or ≤2 V. This is considered a low power for a modulator with plan an MZIM. It can use an applied electric field of at least 233 V/mm, and a driving voltage about 100 V. In Figures 6 and 7, a window of wavelength (633-647) nm is used, with a length of arms L of (2-3) mm. In Figures 8 and 9, a window of wavelength (633-1560) nm is used with a length of arms L of (2-10) mm. In these two cases, the effective factor is the wavelength. Decreasing the wavelength leads to decreasing the applied voltage and half-wave voltage. Therefore, the refractive index also increases to result in a high-quality phase-modulation or intensity modulation, as (20). Furthermore, increasing the refractive index results in a low driving voltage and better performance of the optical modulator. Thus, Figures 6 and 7 are considered a better case of the optical modulators because the case is the real and imaginary parts. In addition, the operation half-wave voltage started from an approximate value of 0.8 V which is a smaller value of half-wave voltage $V\pi$, (i.e., approximately 1.2 V). Also, the optical confinement factor can be used to measure the size of the overlap between the optical field and the electrical field by changing the index of refraction of the LN material through a certain length of the modulator. Utilizing a good confinement factor (large overlap) of about ≤1 unitless, good performance of the modulator can be achieved with a length of the modulator of about 2 mm with applying an electric field of 175 V/mm. Moreover, it achieves an electric field of 233 V/mm by it is poling about 100 V as shown in Figure 10. Eventually, the contribution of this work is to design asymmetric longitudinal MZM by improving the modulation technique. Further, it used a wide window of wavelength from visible-into IR and used a length of arms in mm, see Table 2.

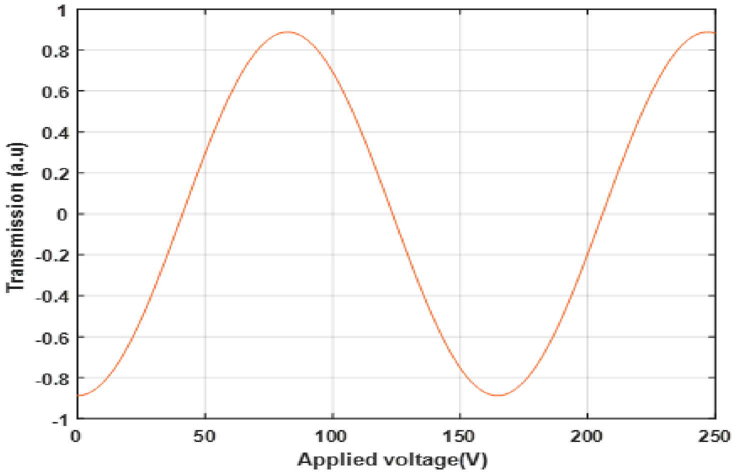

Figure 6. Transmission as function of applied voltage

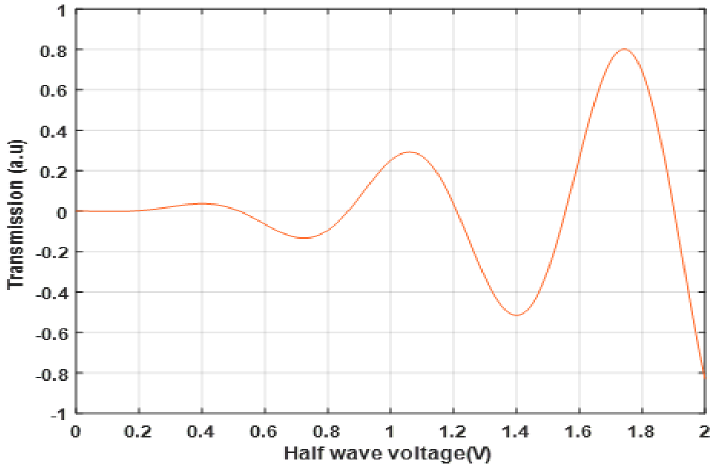

Figure 7. Transmission as function of half wave voltage

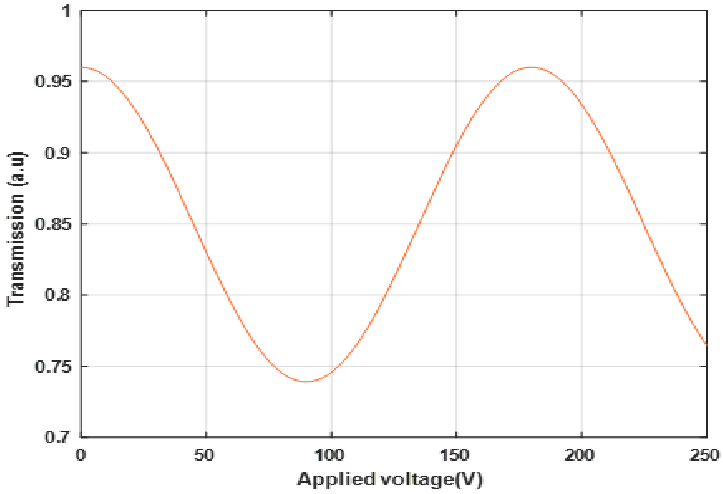

Figure 8. Transmission as function of applied voltage with effect longitudinally uniform push-pull modulator

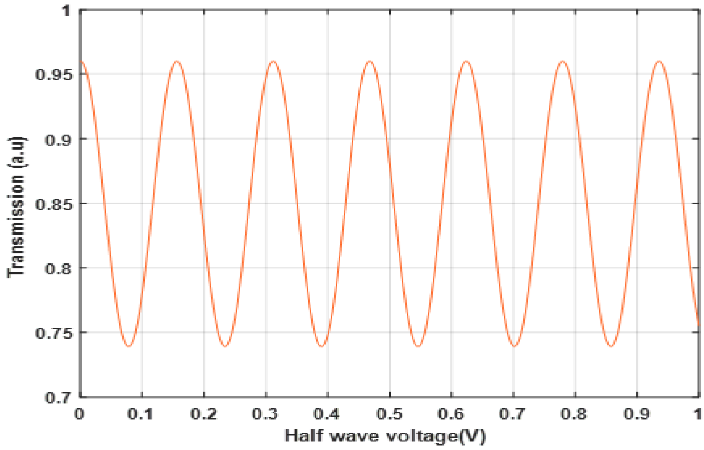

Figure 9. Transmission as function of half wave voltage with effect longitudinally uniform push-pull modulator

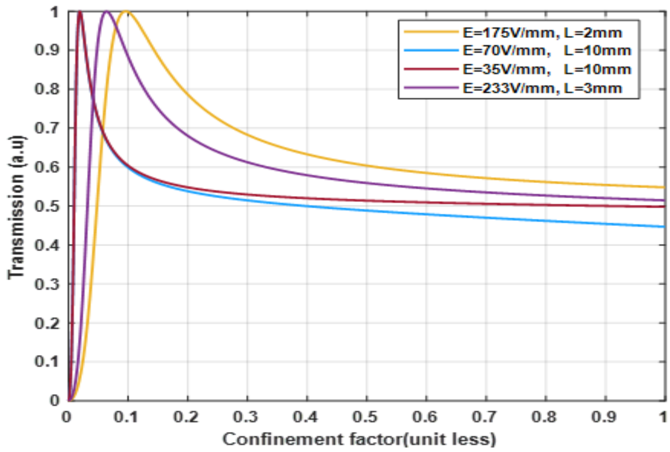

Figure 10. Illustration explains the relation of confinement factor with electric field, optical intensity of light, and length of modulator

Table 2. The comparison between the reference paper [14], [46] and this work

Reference	Δn	L and d	Vπ	ΔØ	E	Γ	Modulator type
[14]	Small L in cm	Large L in cm	Small (1 V)	π	E=V/L	Large	Longitudinal
[46]	Small d in µm	Large d in µm	Large (3.5-4.5 V) Γ increased	π/2	E=V/d	Large	Transvers
This work	Large L in mm	Small L in mm	Small (1.2 V) L in mm	π	E=V/L	Large	Longitudinal

4. CONCLUSION

This paper presented a mathematical model to solve the problems of a narrow window of wavelength for MZM, a large half-wave voltage, and a small optical confinement factor. This designed model was applied using a symmetric push-pull MZIM based on LN material. The proposed structure achieved a wide window of wavelength of 632.8-1560 nm or visible-to-infrared. Furthermore, in this modulator design, three regions of wavelength are accomplished: (632.8-634) nm and (646-647.5) nm, using a short-haul application. In addition, the long-haul applications achieved by the window are 1550-1560 nm. The three windows give a better modulation performance as they give lower attenuation and dispersion. The modulator's accomplishments of better performance and high efficiency also reflected smaller operation half-wave voltage which is about 1.2 V. Where the applied voltage is an appropriate value (i.e. 250 V), by poling on the arms of the modulator. Also, it creates an applied electric field of 233 V/mm by a poling voltage of 100 V. Thus, a good confinement factor of ≤1 (i.e, large overlap) can be obtained when utilizing a small length of the modulator of about 2 mm, and an electric field of 175 V/mm because the large overlap occurs with good tuning between the intensity of light and electric field.

REFERENCES

[1] N. Courjal *et al.*, *Lithium Niobate Optical Waveguides and Microwaveguides*. IntechOpen, Emerging Waveguide Technology, 2018, doi: 10.5772/intechopen.76798.

[2] L. N. Binh, "Lithium niobate optical modulators: Devices and applications," *Journal of Crystal Growth*, vol. 288, no. 1, pp. 180–187, Feb. 2006, doi: 10.1016/j.jcrysgro.2005.12.020.

[3] H. Hichem and B. Djamel, "Comparative between (LiNbO3) and (LiTaO3) in detecting acoustics microwaves using classification," *IAES International Journal of Artificial Intelligence (IJ-AI)*, vol. 8, no. 1, Mar. 2019, doi: 10.11591/ijai.v8.i1.pp33-43.

[4] P. Kolchin, C. Belthangady, S. Du, G. Y. Yin, and S. E. Harris, "Electro-Optic Modulation of Single Photons," *Phys. Rev. Lett.*, vol. 101, no. 10, p. 103601, Sep. 2008, doi: 10.1103/PhysRevLett.101.103601.

[5] K. Noguchi, O. Mitomi, and H. Miyazawa, "Millimeter-wave Ti:LiNbO/sub 3/ optical modulators," *Journal of Lightwave Technology*, vol. 16, no. 4, pp. 615–619, Apr. 1998, doi: 10.1109/50.664072.

[6] M. M. H. Husaini, C. B. M. Rashidi, S. N. Azemi, S. A. Aljunid, and M. S. Anuar, "Optical millimeter wave generation utilizing stimulated brillouin scattering for radio over fiber system," *Indonesian Journal of Electrical Engineering and Computer Science*, vol. 13, no. 2, Feb. 2019, doi: 10.11591/ijeecs.v13.i2.pp818-824.

[7] M. Zhang *et al.*, "Ultra-High Bandwidth Integrated Lithium Niobate Modulators with Record-Low Vπ," in *Optical Fiber Communication Conference Postdeadline Papers (2018), paper Th4A.5*, Mar. 2018, p. Th4A.5, doi: 10.1364/OFC.2018.Th4A.5.

[8] V. K. Singh, A. K. S. Yadav, A. Kumar, and A. Tyagi, "Semiconductor-Optical-Amplifier Mach-Zehnder Interferometer Based Optical Networks," *Indonesian Journal of Electrical Engineering and Computer Science*, vol. 11, no. 1, Jan. 2013.

[9] N. H. Roslan, A. H. Awang, M. H. M. Yusoff, and A. R. M. Zain, "Comparison of lithium niobate and silicon substrate on phase shift and efficiency performance for mach-zehnder interferometer modulator," *Indonesian Journal of Electrical Engineering and Computer Science*, vol. 22, no. 1, Apr. 2021, doi: 10.11591/ijeecs.v22.i1.pp352-360.

[10] L. Chang *et al.*, "Heterogeneous integration of lithium niobate and silicon nitride waveguides for wafer-scale photonic integrated circuits on silicon," *Opt. Lett., OL*, vol. 42, no. 4, pp. 803–806, Feb. 2017, doi: 10.1364/OL.42.000803.

[11] C. Wang *et al.*, "Integrated lithium niobate electro-optic modulators operating at CMOS-compatible voltages," *Nature*, vol. 562, no. 7725, Art. no. 7725, Oct. 2018, doi: 10.1038/s41586-018-0551-y.

[12] A. Boes, B. Corcoran, L. Chang, J. Bowers, and A. Mitchell, "Status and Potential of Lithium Niobate on Insulator (LNOI) for Photonic Integrated Circuits," *Laser and Photonics Reviews*, vol. 12, no. 4, p. 1700256, 2018, doi: 10.1002/lpor.201700256.

[13] A. J. Mercante, S. Shi, P. Yao, L. Xie, R. M. Weikle, and D. W. Prather, "Thin film lithium niobate electro-optic modulator with terahertz operating bandwidth," *Opt. Express, OE*, vol. 26, no. 11, pp. 14810–14816, May 2018, doi: 10.1364/OE.26.014810.

[14] A. Rao and S. Fathpour, "Compact Lithium Niobate Electrooptic Modulators," *IEEE Journal of Selected Topics in Quantum Electronics*, vol. 24, no. 4, pp. 1–14, Jul. 2018, doi: 10.1109/JSTQE.2017.2779869.

[15] L. Arizmendi, "Photonic applications of lithium niobate crystals," *physica status solidi (a)*, vol. 201, no. 2, pp. 253–283, 2004, doi: 10.1002/pssa.200303911.

[16] P. Rabiei, J. Ma, S. Khan, J. Chiles, and S. Fathpour, "Heterogeneous lithium niobate photonics on silicon substrates," *Opt. Express, OE*, vol. 21, no. 21, pp. 25573–25581, Oct. 2013, doi: 10.1364/OE.21.025573.

[17] S. Bogdanov, M. Y. Shalaginov, A. Boltasseva, and V. M. Shalaev, "Material platforms for integrated quantum photonics," *Opt. Mater. Express, OME*, vol. 7, no. 1, pp. 111–132, Jan. 2017, doi: 10.1364/OME.7.000111.

[18] M. Berciano *et al.*, "Fast linear electro-optic effect in a centrosymmetric semiconductor," *Commun Phys*, vol. 1, no. 1, Oct. 2018, doi: 10.1038/s42005-018-0064-x.

[19] K. Alexander *et al.*, "Nanophotonic Pockels modulators on a silicon nitride platform," *Nat Commun*, vol. 9, no. 1, Aug. 2018, doi: 10.1038/s41467-018-05846-6.

[20] H. Takagi, R. Maeda, N. Hosoda, and T. Suga, "Room-temperature bonding of lithium niobate and silicon wafers by argon-beam surface activation," *Appl. Phys. Lett.*, vol. 74, no. 16, pp. 2387–2389, Apr. 1999, doi: 10.1063/1.123860.

[21] A. Azmi, K. a. A. Seman, and K. Y. Lau, "Breakdown characteristics of polyethylene/silicon nitride nanocomposites," *TELKOMNIKA (Telecommunication Computing Electronics and Control)*, vol. 17, no. 4, Aug. 2019, doi: 10.12928/telkomnika.v17i4.12754.

[22] E. L. Wooten *et al.*, "A review of lithium niobate modulators for fiber-optic communications systems," *IEEE Journal of Selected Topics in Quantum Electronics*, vol. 6, no. 1, pp. 69–82, Jan. 2000, doi: 10.1109/2944.826874.

[23] M. M. Kareem, S. A. S. Lafta, H. F. Hashim, R. K. Al-Azzawi, and A. H. Ali, "Analyzing the BER and optical fiber length performances in OFDM RoF links," *Indonesian Journal of Electrical Engineering and Computer Science*, vol. 23, no. 3, pp. 1501-1509, Sep. 2021, doi: 10.11591/ijeecs.v23.i3.pp1501-1509.

[24] M. M. R. Howlader, T. Suga, and M. J. Kim, "Room temperature bonding of silicon and lithium niobate," *Appl. Phys. Lett.*, vol. 89, no. 3, p. 031914, Jul. 2006, doi: 10.1063/1.2229262.

[25] V. E. Stenger *et al.*, "Low Loss and Low Vpi Thin Film Lithium Niobate on Quartz Electro-optic Modulators," in *2017 European Conference on Optical Communication (ECOC)*, Sep. 2017, pp. 1–3, doi: 10.1109/ECOC.2017.8346144.

[26] P. O. Weigel *et al.*, "Lightwave Circuits in Lithium Niobate through Hybrid Waveguides with Silicon Photonics," *Sci Rep*, vol. 6, no. 1, Mar. 2016, doi: 10.1038/srep22301.

[27] A. Guarino, G. Poberaj, D. Rezzonico, R. Degl'Innocenti, and P. Günter, "Electro–optically tunable microring resonators in lithium niobate," *Nature Photon*, vol. 1, no. 7, Jul. 2007, doi: 10.1038/nphoton.2007.93.

[28] V. Stenger *et al.*, "Integrated RF photonic devices based on crystal ion sliced lithium niobate," in *Terahertz, RF, Millimeter, and Submillimeter-Wave Technology and Applications VI*, Mar. 2013, vol. 8624, pp. 96–103, doi: 10.1117/12.2004623.

[29] L. Cai, Y. Kang, and H. Hu, "Electric-optical property of the proton exchanged phase modulator in single-crystal lithium niobate thin film," *Opt. Express, OE*, vol. 24, no. 5, pp. 4640–4647, Mar. 2016, doi: 10.1364/OE.24.004640.

[30] V. Stenger *et al.*, "Engineered Thin Film Lithium Niobate Substrate for High Gain-Bandwidth Electro-optic Modulators," in *CLEO: 2013 (2013), paper CW3O.3*, Jun. 2013, p. CW3O.3, doi: 10.1364/CLEO_SI.2013.CW3O.3.

[31] A. Rao *et al.*, "High-performance and linear thin-film lithium niobate Mach–Zehnder modulators on silicon up to 50 GHz," *Opt. Lett., OL*, vol. 41, no. 24, pp. 5700–5703, Dec. 2016, doi: 10.1364/OL.41.005700.

[32] M. M. A. Eid, A. S. Seliem, A. N. Z. Rashed, A. E.-N. A. Mohammed, M. Y. Ali, and S. S. Abaza, "High speed pulse generators with electro-optic modulators based on different bit sequence for the digital fiber optic communication links," *Indonesian Journal of Electrical Engineering and Computer Science*, vol. 21, no. 2, pp. 957-967, Feb. 2021, doi: 10.11591/ijeecs.v21.i2.pp957-967.

[33] M. J. Mohsin and I. A. Murdas, "Designing an optical frequency comb generator for visible light communication applications," *International Journal of Electrical and Computer Engineering (IJECE)*, vol. 12, no. 1, Feb. 2022, pp. 471-477, doi: 10.11591/ijece.v12i1.pp471-477.

[34] P. O. Weigel *et al.*, “Bonded thin film lithium niobate modulator on a silicon photonics platform exceeding 100 GHz 3-dB electrical modulation bandwidth,” *Opt. Express, OE*, vol. 26, no. 18, pp. 23728–23739, Sep. 2018, doi: 10.1364/OE.26.023728.
[35] A. J. Mercante, P. Yao, S. Shi, G. Schneider, J. Murakowski, and D. W. Prather, “110 GHz CMOS compatible thin film LiNbO3 modulator on silicon,” *Opt. Express, OE*, vol. 24, no. 14, pp. 15590–15595, Jul. 2016, doi: 10.1364/OE.24.015590.
[36] X. Wang, P. O. Weigel, J. Zhao, M. Ruesing, and S. Mookherjea, “Achieving beyond-100-GHz large-signal modulation bandwidth in hybrid silicon photonics Mach Zehnder modulators using thin film lithium niobate,” *APL Photonics*, vol. 4, no. 9, p. 096101, Sep. 2019, doi: 10.1063/1.5115243.
[37] M. Li, J. Ling, Y. He, U. A. Javid, S. Xue, and Q. Lin, "Lithium niobate photonic-crystal electro-optic modulator," Nature Communications, vol. 11, 2020. doi: 10.1038/s41467-020-17950-7.
[38] T. A. Maldonado, “Chapter 13 electro-optic modulators,” in *kipdf.com*, vol. 2, Texas, 1995, pp. 13.1-13.35, [Online], Available: https://kipdf.com/chapter-13-electro-optic-modulators_5b12679f7f8b9a525a8b45b3.html
[39] M. Polyanskiy, “Optical constants of LiNbO3 (Lithium niobate),” 2008. [Online], Available: https://refractiveindex.info/?shelf=main&book=LiNbO3&page=Zelmon-e.
[40] J. L. Casson *et al.*, “Electro-optic coefficients of lithium tantalate at near-infrared wavelengths,” *J. Opt. Soc. Am. B, JOSAB*, vol. 21, no. 11, pp. 1948–1952, Nov. 2004, doi: 10.1364/JOSAB.21.001948.
[41] H. Oulachgar, L. Chrostowski, and R. Bojko, *Silicon Photonics Design, Fabrication and Data Analysis*. 2015. doi: 10.13140/RG.2.2.36759.29609.
[42] V. Palodiya and S. K. Raghuwanshi, “Performance Study of optical Modulator based on electrooptic effect,” *J. Phys.: Conf. Ser.*, vol. 735, no. 1, p. 012071, Aug. 2016, doi: 10.1088/1742-6596/735/1/012071.
[43] Z. Ma, M. H. Tahersima, S. Khan, and V. J. Sorger, “Two-Dimensional Material-Based Mode Confinement Engineering in Electro-Optic Modulators,” *IEEE Journal of Selected Topics in Quantum Electronics*, vol. 23, no. 1, pp. 81–88, Jan. 2017, doi: 10.1109/JSTQE.2016.2574306.
[44] G. Hagn, “Electro-optic effects and their application in indium phosphide waveguide devices for fibre optic access networks,” Doctoral Thesis, ETH Zurich, 2001, doi: 10.3929/ethz-a-004353336.
[45] A. S. Abdullah and S. A. Hbeeb, “The ordinary negative changing refractive index for estimation of optical confinement factor,” *International Journal on Smart Sensing and Intelligent Systems*, vol. 15, no. 1, Jan. 2022, doi: 10.2478/ijssis-2022-0009.
[46] T. Ren *et al.*, “An Integrated Low-Voltage Broadband Lithium Niobate Phase Modulator,” *IEEE Photonics Technology Letters*, vol. 31, no. 11, pp. 889–892, Jun. 2019, doi: 10.1109/LPT.2019.2911876.

BIOGRAPHIES OF AUTHORS

Sadeq Adnan Hbeeb received his B.Eng. degree in electrical and electronic engineering, and M.Eng. degree in laser and optoelectronic engineering in 2002 and 2007 respectively from University of Technology/Baghdad-Iraq. His research interests include photonics system, optical devices, and opto-electronic system. He can be contacted at email: sadeq.hbeeb@gmail.com.

Ahmad Sulaiman Abdullah received his B.Sc. degree in Electrical and Electronic Engineering in 2000, and M.Sc. degree in Laser and Optoelectronics engineering in 2008 from the University of Technology, Baghdad, Iraq. He completed his Ph.D. degree in 2018 from the Altınbaş University in Istanbul, Turkey. His research areas of interest are biomedical image processing, optical communication, photonics system, and digital signal processing. He can be contacted at email: ahmed.alogaidi28@gmail.com.

Haider Ali Jasim Alshamary received his master’s degree in electronics engineering from the University of Technology-Iraq in 2007. He worked as an assistant teacher at the University of Diyala until 2011. He received his Ph.D. degree from the Department of Computer and Electrical Engineering at the University of Iowa in May 2017. Since then, he is working as a lecturer at the University of Diyala in the communication engineering department. His research interests are massive MIMO, channel estimation and data detection of communication systems, signal processing, and electronic circuit design. He can be contacted at email: haider.alshamary@uodiyala.edi.iq.